[Supporting Information (SI) to accompany:]

One Electron Changes Everything. A Multi-Species Copper Redox Shuttle for Dye-Sensitized Solar Cells

W. L. Hoffeditz[a], M. J. Katz[a,d], P. Deria[a,e], G. E. Cutsail III[a,f], , M. J. Pellin[a,b], O. K. Farha*[,a,c], J. T. Hupp*[,a,b].

[a]*Department of Chemistry, Northwestern University, 2145 Sheridan Road, Evanston, Illinois 60208, United States.*

[b]*Material Science Division, Argonne National Laboratory, 9700 South Cass Avenue, Argonne, Illinois 60439, United States.*

[c]*Department of Chemistry, Faculty of Science, King Abdulaziz University, Jeddah, Saudi Arabia*

[d]*Current address: Department of Chemistry, Memorial University of Newfoundland, St. John's, NL A1B 3X7, Canada.*

[e]*Current address: Department of Chemistry and Biochemistry, Southern Illinois University-Carbondale, 1245 Lincoln Drive, Carbondale, IL 62901, United States.*

[f]*Current address: Max-Planck Insititut für Chemische Energiekonversion, Stiftstrasse 34 – 36, D-45470 Mülheim an der Ruhr, Germany*

Table of Contents

Section S1. EPR spectral parameters and simulations

Table S1. Copper EPR Spectral Parameters

	$g_\perp$	$g_\parallel$	$A(\mathrm{Cu})_\perp$[a]	$A(\mathrm{Cu})_\parallel$	$A(^{14}\mathrm{N})_\perp$	$A(^{14}\mathrm{N})_\parallel$
$Cu(CF_3SO_3)_4^{2+}$	2.085	2.432	35	340	–	–
Cu(PDTO)	2.0384	2.168	75	512	50.5 38.5	38 38
Cu(PDTO)+TBP[b]	2.054	2.255	47	555	39	30.5
Cu(TBP)[b]	2.054	2.255	47	555	39	30.5
Cu(TBP) (powder)	2.05	2.25	80	560	–	–

[a] All hyperfine values are given in units of MHz

[b] Simulated with 5 equivalent nitrogens (^{14}N) nuclei

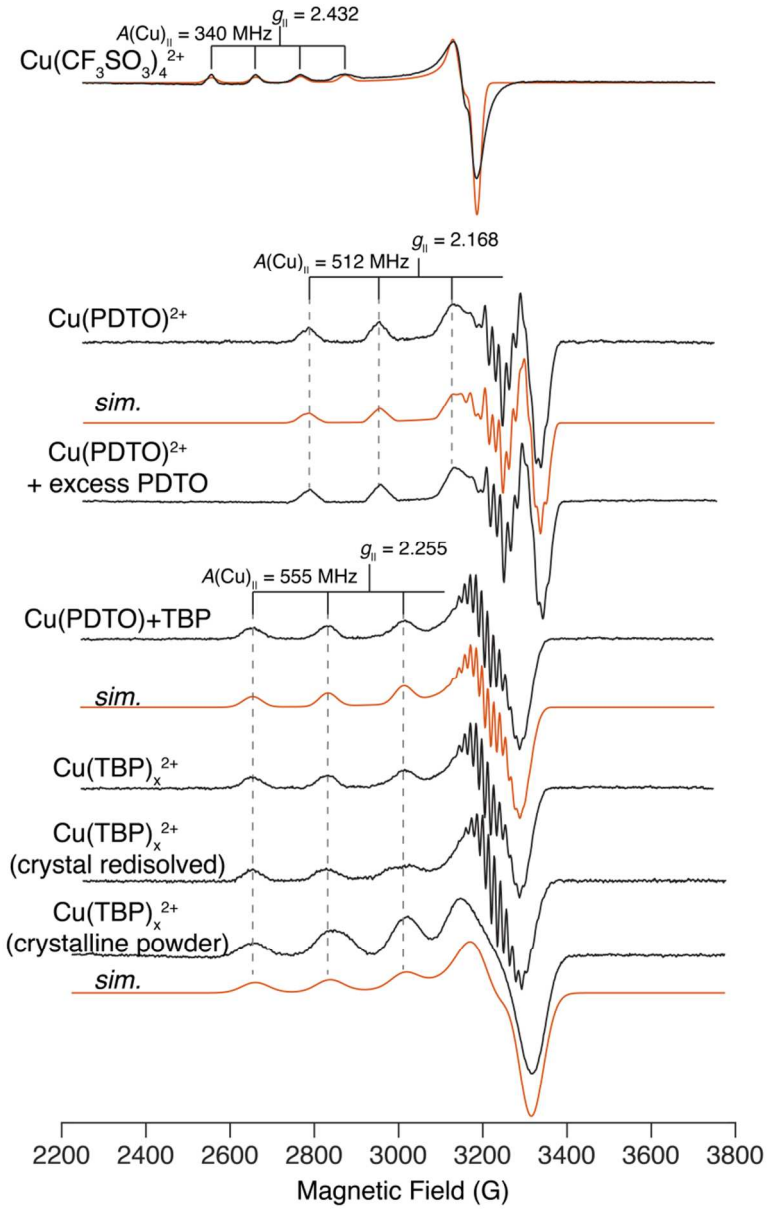

Figure S1. All EPR spectra were collected under conditions described of Figure 5. Simulation parameters are given in Table S1.

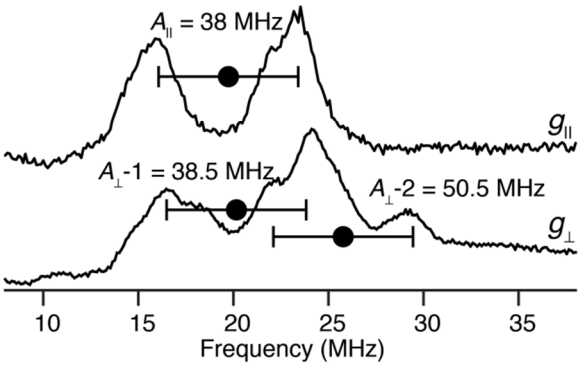

Figure S2. Q-band (34.93 GHz) pulsed Davies ENDOR spectra of $Cu(PDTO)^{2+}$ at $g_{||}$ (11680 G) and $g_{\perp}$ (12140 G) taken at 2 K collected on instrumentation previously described.[1] The observed ^{14}N couplings are $A/2$ centered (circles) split by $2\nu_n$ (goalposts). At $g_{||}$, only a single doublet is observed corresponding to overlapping $A_{||}$ for two nitrogens. At $g_{\perp}$, two nitrogens are resolved with couplings of $A(^{14}N\text{-}1)_{\perp}$ = 38.5 and $A(^{14}N\text{-}2)_{\perp}$ = 50.5 MHz. These ^{14}N hyperfine coupling values are employed in the corresponding X-band EPR simulation of $Cu(PDTO)^{2+}$. *Conditions.* Pulse sequence: $\pi - T_{RF} - \pi/2 - \tau - \pi - \tau$ –echo; π = 80 ns; τ = 600 ns; T_{RF} = 15 μs; repetition time = 20 ms.

Section S2. UV-Vis spectra for PDTO and TBP ligand titration.

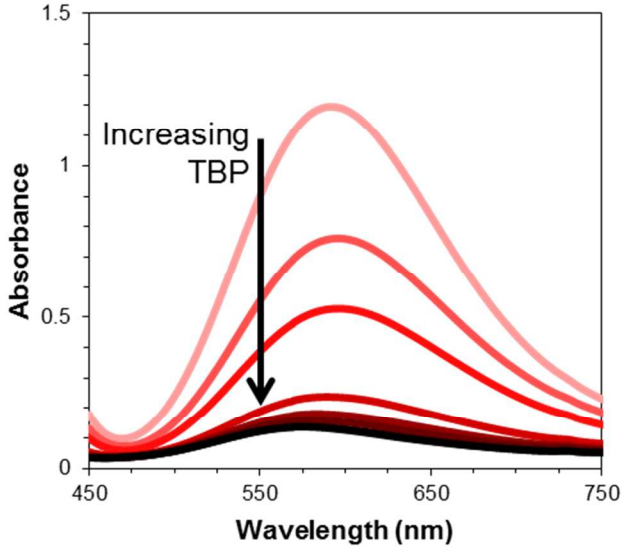

Figure S3. UV-Vis spectroscopy of the $Cu(PDTO)^{2+}$ complex in acetonitrile titrated with 4-*tert*-butylpyridine (TBP) corresponding to Figure 5 in the main text. The initial, ≥1 Abs. U. peak contains no TBP. As TBP is added in one equivalent to Cu amounts, the absorbance magnitude begins to decrease, eventually leveling off around six equivalents.

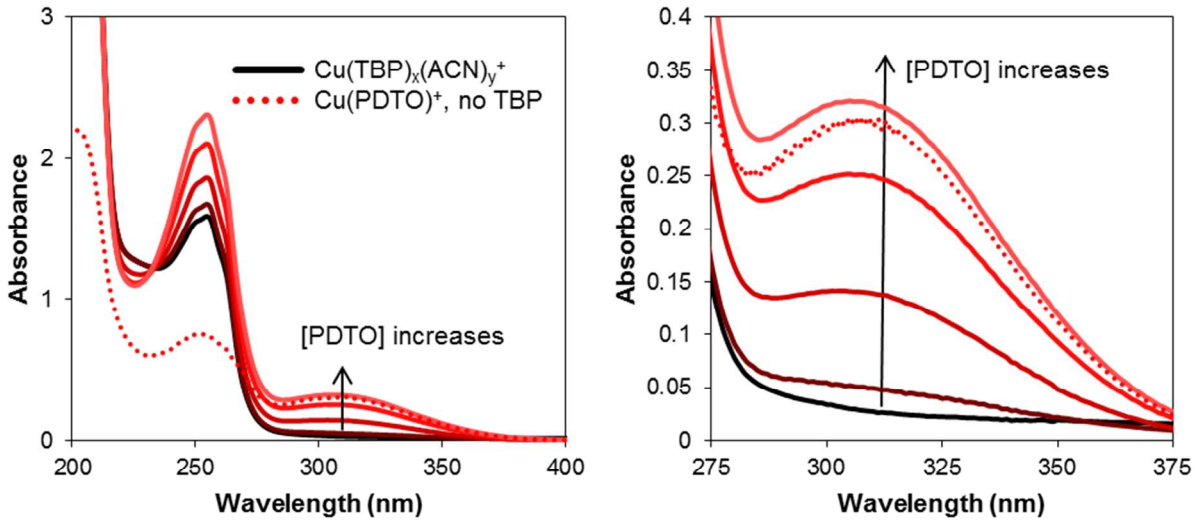

Figure S4. UV-Vis spectra of tetrakisacetonitrile copper(I) hexafluorophosphate in the presence of 10 mole equivalents TBP titrated with PDTO. The figure on the right is a magnified section of the figure on the left. The solid traces begin with no PDTO present (black), then progress to 1:100 PDTO:TBP ratio (1:10 PDTO:Cu ratio), 4:100, 7:100, and finally 1:10 PDTO:TBP (1:1 PDTO:Cu). Of particular importance is the immediate reappearance of the absorption feature associated with sulphur-copper bonds near 315 nm, even when TBP is present in 100X higher concentration. The dotted red line represents $Cu(ACN)_4^+$ in the presence of one mole equivalent of PDTO and the absence of TBP. The large difference in absorbance at ~250 is likely due to the location of a main absorbance feature of TBP in the same area (see Figure 7 in main text).

Section S3. Dark current/voltage curves and open circuit voltage decay plots for I_3^- and $Co(bpy)_3^{3+}$.

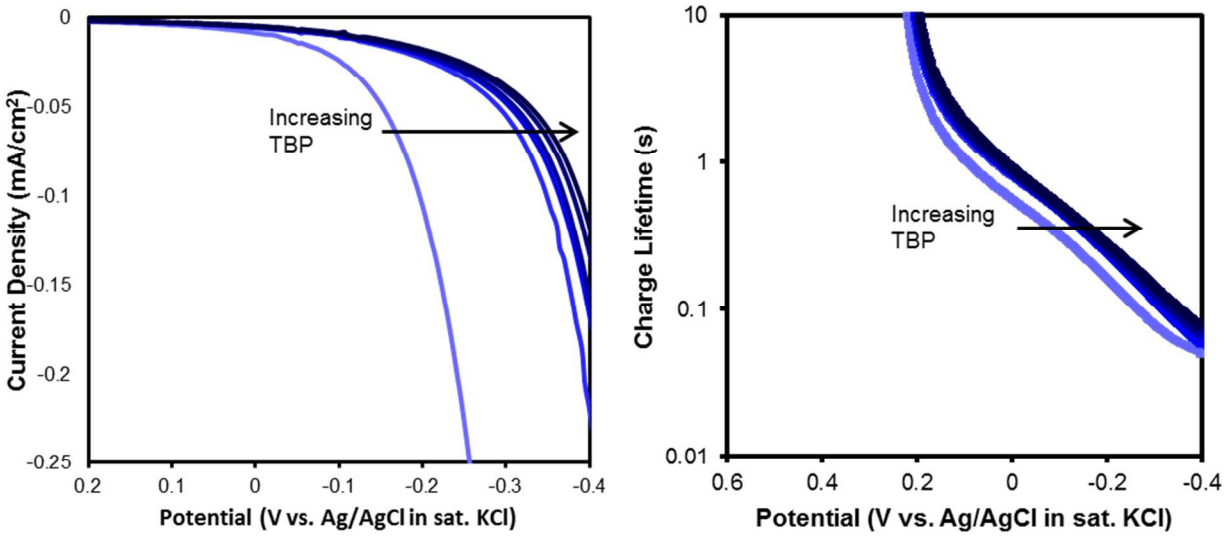

Figure S5. Dark current/voltage curves (left) and open circuit photovoltage decay (OCVD) plots (right) for 0.5 N I_3^- in acetonitrile in the presence of increasing amounts of TBP. For the dark current curves, a large, initial increase in onset potential of approximately 200 mV is observed upon the addition of 1 mole equivalent of TBP. Further additions of TBP (2, 3, 5, 8, and 10 mole equivalents are shown, with 10 mole equivalents being roughly equal to the standard DSC operating concentration of TBP) have a minimal effect (~50 mV) on dark current onset potential. This effect is likely entirely due to surface association of TBP. OCVD plots give similar results, with the initial addition of TBP causing a small increase in charge lifetime and subsequent additions having a much smaller effect. Again, this effect is likely due to surface association of TBP with TiO_2. These effects contrast strongly with those observed with the copper shuttle, supporting the idea of interaction directly between the copper shuttle and TBP.

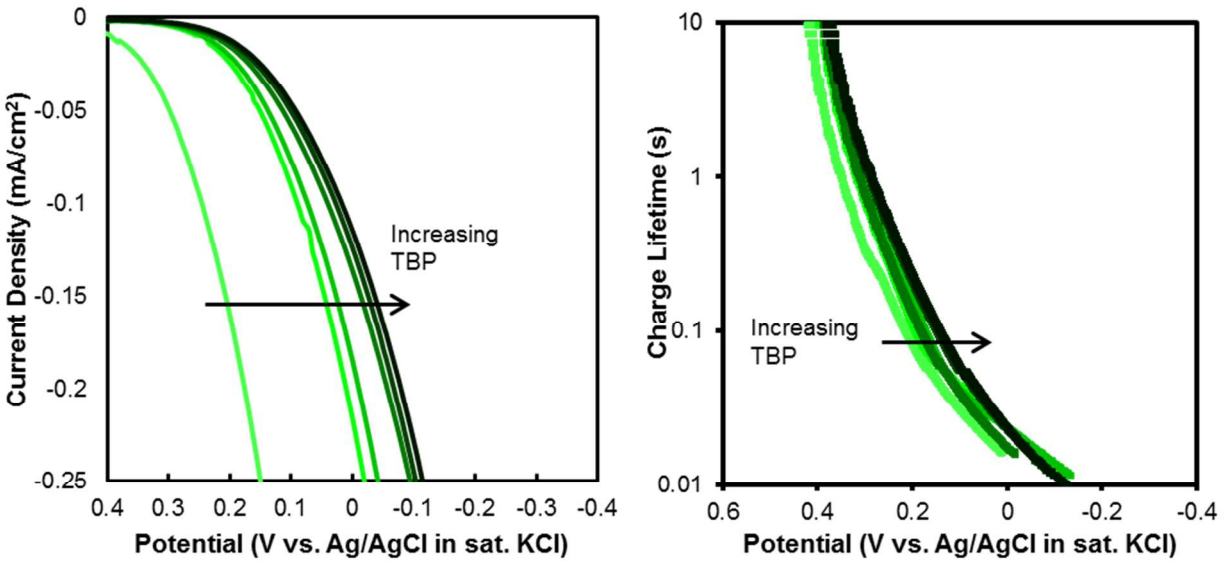

Figure S6. Dark current/voltage curves (left) and open circuit photovoltage decay (OCVD) plots (right) for 0.5 N $Co(bpy)_3^{3+}$ in acetonitrile in the presence of increasing amounts of TBP. Similar to the trend observed with triiodide, the initial addition of 1 mole equivalent TBP has the largest effect on dark current onset. Subsequent additions to reach 2, 3, 5, 8, and 10 equivalents of TBP again had a significantly smaller effect on dark current onset, likely due to TBP association with TiO_2. OCVD plots for $Co(bpy)_3^{3+}$ also show a similar trend as observed with I_3^-. Together with the data in Figure S1 for I_3^-, these results strongly support association of TBP with the copper(II) center as opposed to TBP only associating with TiO_2.

Section S4. Comparison of JV curves using high area and standard Pt dark electrodes**.**

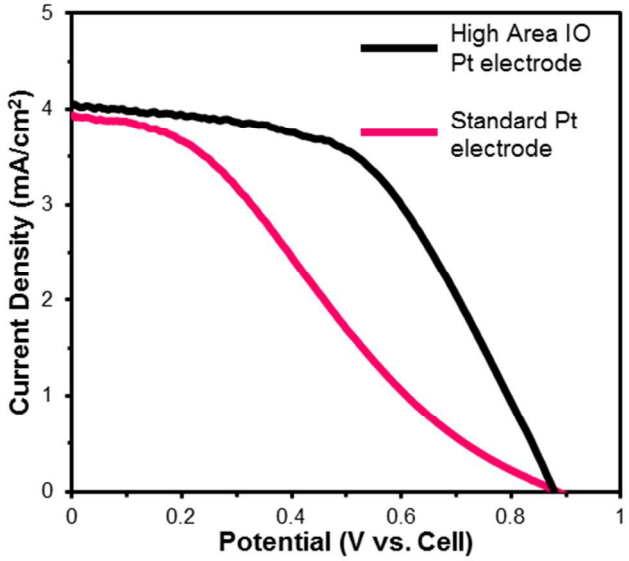

Figure S7. Comparison of JV curves utilizing a standard Pt dark electrode fabricated by the thermal decomposition of H_2PtCl_6 (pink) and a high area, Pt coated inverse opal dark electrode (black). The slow reduction kinetics of the $Cu(TBP)_{4+x}(ACN)_y^{2+}$ complex results in a poor fill factor due to charge transfer resistance at the dark electrode. The high area of a Pt coated inverse opal film remedies this problem by increasing the rate of the reaction via increasing the number of reactive sites, explained in detail in a previous publication.[2]

Section S5. Front-side/back-side IPCE plot.

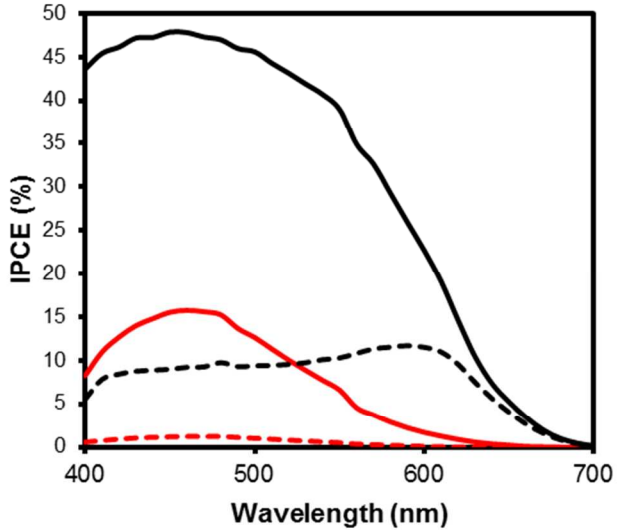

Figure S8. Front-side (solid lines) and back-side (dashed lines) incident photon-to-electron conversion efficiency (IPCE) for devices with no added 4-*tert*-butylpyridine (TBP, red traces) and 0.5 M added TBP (black traces). At an illumination wavelength of 500 nm the photoelectrode features an absorbance of *ca.* 3 (see Figure S9 below). The photocurrent due to back-side illumination at this wavelength is only about 20% of the value obtained with front-side illumination. Thus, the first 80% of absorbed photons appear to be generated to distant from the current collector to contribute to J_{sc}. Assuming uniform loading of dye on the photoelectrode, 80% of the incident photons at 500 nm will be absorbed within the first 1.9 microns of the electrode. For back-side illumination, therefore, electrons generated at any distance beyond 1.9 microns are likely to be collected by the conductive glass material sited at the opposite side of the ~8-micron-thick TiO_2 electrode.

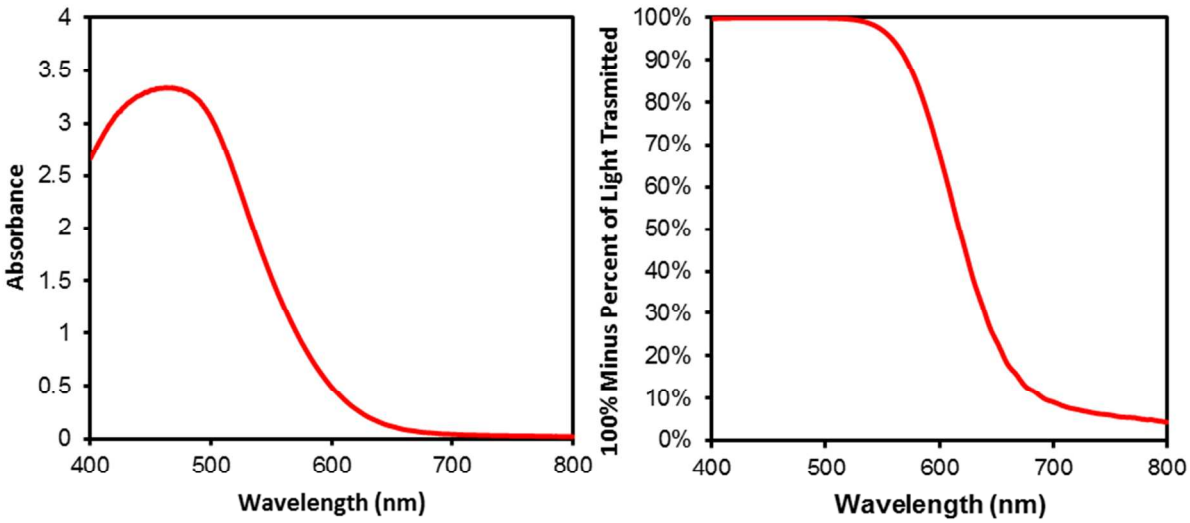

Figure S9. Light harvesting characteristics of Carbz-PAHTDTT dye on ~ 8 micrometer thick TiO_2 films plotted as absorbance vs. wavelength (left) and as a percentage of light absorbed (right).

Section S6. J-V curve and CV with $Cu(TBP)_{4+x}(ACN)_y^{2+/+}$.

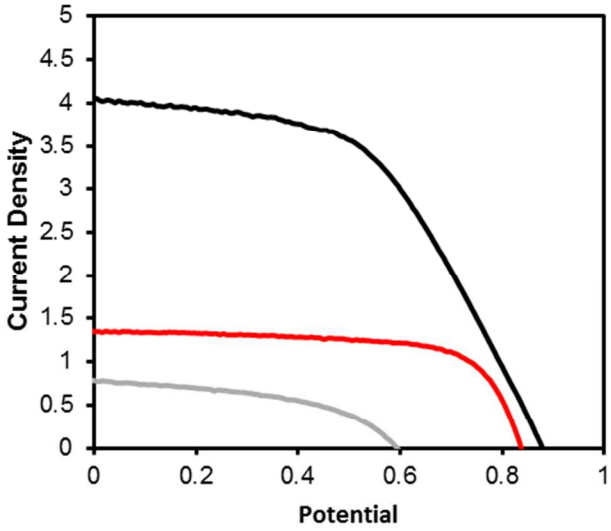

Figure S10. J-V curve of $Cu(TBP)_{4+x}(ACN)_y^{2+/+}$ (gray line) utilized as a redox shuttle in a DSC. PDTO is not present in solution in this device. For comparison, the J-V curves obtained from the $Cu(PDTO)^{2+/+}$ shuttle (red line) and the mixed system $Cu(TBP)_{4+x}(ACN)_y^{2+}/Cu(PDTO)^{+}$ shuttle (black line) are also shown.

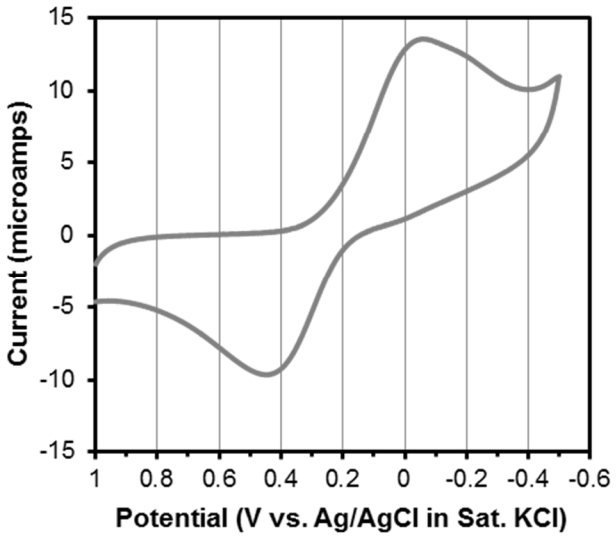

Figure S11. Cyclic voltammagram of $Cu(TBP)_{4+x}(ACN)_y^{2+/+}$.

Section S7. References

(1) Davoust, C. E.; Doan, P. E.; Hoffman, B. M. Q-Band Pulsed Electron Spin-Echo Spectrometer and Its Application to Endor and Eseem. *Journal of Magnetic Resonance, Series A* **1996,** *119*, 38-44.

(2) Hoffeditz, W. L.; Katz, M. J.; Deria, P.; Martinson, A. B. F.; Pellin, M. J.; Farha, O. K.; Hupp, J. T. High-Surface-Area Architectures for Improved Charge Transfer Kinetics at the Dark Electrode in Dye-Sensitized Solar Cells. *ACS Appl. Mater. Interfaces* **2014,** *6*, 8646-8650.